

Galaxies at High Redshift

Garth Illingworth

UCO/Lick Observatory, Astronomy and Astrophysics Department, University of California, Santa Cruz, CA 95064

October 15, 1999

Abstract. Within just the last few years, we have advanced from knowing only a few galaxies at $z > 2$ to having redshifts for nearly 1000 $z \sim 2$ –5 objects. The majority of this sample has been detected through the photometric “drop-out” technique used so successfully by Steidel and his collaborators. In addition, a handful of objects have already been detected at $z > 5$, and we may already have a few objects at $z > 6$! These data, plus that at $z < 2$ have resulted in a characterization of the star formation history of the universe, commonly known as the “Madau plot”, which gives SFR per comoving volume *vs* redshift from the present day at $z = 0$ to $z \sim 5$. Recently, we have realized that dust has significantly affected our SFR estimates for the objects that have been detected in the optical, and have developed approaches to correct for that extinction. We now also have increasingly good evidence that a substantial fraction ($>50\%$?) of the high redshift star formation occurs in dust-enshrouded starbursts that were detected at $850\ \mu\text{m}$ with a submm bolometer SCUBA on the JCMT telescope. These objects will typically be too faint to detect and measure redshifts in the optical, though those that can have already provided valuable constraints. The highest redshift objects at $z \sim 5$ and beyond are intriguing sources, but test even the limits of Keck and of HST. The detailed study of such sources may well only be practical for gravitationally-lensed objects, where the high magnification allows for a much more detailed study of the proto-galaxy’s structure, until even larger space-based (NGST) and ground-based (30-m plus) telescopes are developed.

Keywords: High Redshift Galaxies, Starburst Galaxies

1. Introduction

Two new telescope/instrument combinations came on line in the mid 1990s that resulted in a dramatic increase in our ability to observe distant galaxies. The refurbishment mission that added the WFPC2 camera to HST, along with its corrective optics, plus the commissioning of the Low Resolution Imaging Spectrograph on the Keck I telescope provided new, and complementary, capabilities for observing faint, small, low surface brightness objects. This led to a remarkable resurgence of interest in distant galaxies, and a large increase in the statistical and quantitative veracity of the resulting data.

HST WFPC2 imaging has provided us opportunities to resolve distant galaxies, and extend our morphological and structural characterizations to galaxies at much higher redshift – the limitation now is



© 2000 Kluwer Academic Publishers. Printed in the Netherlands.

largely one of S/N due to the effect of the cosmological $(1+z)^4$ surface brightness dimming and to the (often) large photometric K -corrections due to the rest frame shift into the UV. Some of the best examples of the imaging capabilities of HST have been seen in the multi-color images of the HDF and the “Groth” Survey strip in 1995, and the HDF-S in 1998, and in the deep images of many intermediate redshift (i.e., $z \sim 0.2$ –1) clusters.

The multi-slit spectroscopy from Keck with the LRIS spectrograph has proven to be an ideal complement of the the HST imaging, allowing 30–40 galaxy redshifts to be measured at once to fainter than $I \sim 25$. With Keck plus LRIS it has become possible to routinely derive redshifts for objects several magnitudes fainter than was practical in major (and important) surveys carried out earlier this decade on 4-m class telescopes (e.g., the CFRS, Lilly et al. 1995).

The major developments of the last few years are:

- (1.) — the measurement of large numbers of redshifts for $z \sim 3$ –4 galaxies by Steidel and collaborators;
- (2.) — the identification of several strongly-lensed (and hence highly-magnified) $z \sim 2$ –5 galaxies;
- (3.) — the detection of a number of $z > 5$ galaxies;
- (4.) — the characterization of the star formation history of the universe by Madau and others (the “Madau” plot – SFR *vs* redshift);
- (5.) — the recognition of the impact of dust on the UV fluxes from high redshift galaxies;
- (6.) — the discovery of distant galaxies that are strong submm sources with the JCMT SCUBA submm detector.
- (7.) — the utilization of increasingly more accurate photometric redshifts;

The improvements that are planned for HST imaging with the ACS (the new Advanced Camera), which will provide a gain of $10\times$ in the area-throughput product (the figure-of-merit most appropriate for imaging surveys), and the dramatic increase in the numbers of 6.5-m to 10-m ground-based telescopes with their next generation optical and near-IR multi-object spectrographs will lead to an even greater rate of progress in the high redshift galaxy field within just a few years.

1.1. ISSUES/QUESTIONS

While progress on distant galaxies has been rapid, there are a number of outstanding questions about the highest redshift objects (those at $z > 2$) that are the center of a number of debates. Examples of these are (i) what is the effect of dust on the SFR derived from the rest frame UV SED and flux measurements of $z > 2$ galaxies, (ii) what are

the redshifts of the SCUBA submm sources, (iii) what differentiates the optically-detected starbursts from the highly-obscured, submm sources, (iv) what are the masses of the $z \sim 2-5$ objects, (v) when did the first major star-formation events take place (thus forming the first metals), (vi) what are the physical conditions in high redshift star-forming galaxies, (vii) by what processes, and on what timescales, were the galaxies we see today assembled, and (viii) how do those timescales compare to the timescales for when the bulk of the stars were made?

These questions, and the issues they raise, will be noted during the discussion of the results that are presented in the main body of this paper, and are issues that are encompassed in many discussions of galaxy formation and evolution. As an introduction to developments in high redshift galaxies, and to provide a context for much of the later discussion, a number of items are highlighted first, including (i) timescales, (ii) the recent baryon census, (iii) the photometric “drop-out” technique that has been used so successfully to find high redshift galaxies, (iv) the representation of the star formation history of the universe through what has become to be known as the “Madau” plot, and (v) the importance of the HST deep imaging fields.

These are followed by more detailed discussions of the results on (i) $z \sim 2-5$ galaxies, (ii) the SCUBA results, (iii) the latest detections of the very youngest $z > 5$ galaxies, and (iv) the importance of strongly-lensed sources. Finally, a few comments are made about the future capabilities that will provide the observational framework for the further development of this field, and an assessment of some of the key issues about distant galaxies.

2. Timescales

It is valuable when thinking about distant galaxies to be calibrated on the timescales involved. Based on a reasonable set of numbers, i.e., an open cosmology with $H_0 = 65$ and $q_0 = 0.05$, $t_0 = 15$ Gyr, with the lookback time at $z \sim 1$ is about 50% of t_0 , while the lookback time to $z = 3$ is about 11 Gyr. Or, in a way that is better for thinking about formation timescales, the time since recombination to $z = 10$ is about 1.4 Gyr, to $z = 5$ is about 2.6 Gyr and to $z = 3$ is about 3.9 Gyr. The timescales grow somewhat longer with a lambda-universe, with $\Omega_\Lambda = 0.7$ and $\Omega_m = 0.3$, and dramatically shorter for an Einstein-de Sitter $\Omega_m = 1$ cosmology (giving a rather unrealistically short timescale for galaxy development by $z \sim 5$ of < 1 Gyr!).

3. Baryon Census

A valuable framework for thinking about galaxy development was provided recently by Fukugita, Hogan and Peebles (1998). Taking a wide variety of data sources, they did a census of the baryons at both low and high redshift. While there are significant uncertainties associated with these estimates, they do provide a useful framework for constraining where the mass is in galaxies by type. For example, the low redshift census of the baryons in stars in galaxies shows that the dominant sink of baryons in galaxies integrated over all time t_0 is spheroids. Ellipticals and the bulges of disk systems currently contain, in their stellar population, about 63% of the baryonic mass that is in galaxies (where this baryonic component is considered to be that in stars, stellar evolution end-products, or gas in the galaxy). All disks contain only about 21% of the baryonic mass, while the extremely numerous late type, and, typically, lower luminosity, galaxy population only has 2% of the baryonic mass in stars. The latter mass fraction is small even compared the gas that now remains in galaxies. The gas in galaxies comprises 15% of the total baryonic mass (integrated over all types). Thus a characterization of the star formation history of the universe is largely a description of the formation of spheroid populations, and secondarily, of disks, though if the timescales are quite different, one could still have a period where the dominant process is disk formation.

4. The Photometric “Drop-Out” Technique

The Lyman break photometric “drop-out” technique was first utilized for the detection of high redshift quasars, but was then much more finely tuned as a detection technique for high redshift galaxies by Steidel and his collaborators in the mid-1990s. The technique relies on the large break in the continuum flux from an object that occurs at the 912 Å Lyman limit from neutral hydrogen absorption in the line-of-sight. Multi-band images of a field containing high redshift galaxies can be used to identify those objects that have very red colors as a result of the redshifted Lyman limit falling between any two filters. The technique is refined by having multiple filters that also can detect the smaller break at $L\alpha$ (1216 Å), and the rather blue continuum longwards of $L\alpha$.

As first used extensively by Steidel et al. (1996) the technique was used to detect $z \sim 3$ objects by their lack of flux in the U-band (hence the descriptor “U-band drop-outs”). The technique was often applied by using three or four filters and defining a region in the two-color plane in which such “drop-outs” were most likely to occur. Steidel and

his collaborators used UGR ground-based images, while, for the HDF, the four band images allowed the use of a plane that was essentially $(U - B)$ *vs* $(V - I)$. Examples of the two-color plane and the selection function are given also in Dickinson (1998), as is a very instructive visual representation of the “drop-out” technique for a galaxy at $z = 3$.

This technique has proved to be remarkably useful for detecting $z > 2$ galaxies with ground (and space) imaging in the “optical” (~ 0.3 – $1 \mu\text{m}$). A key advantage of this technique is that it is essentially free of selection effects, with little contamination from low redshift objects. All high redshift objects above a given magnitude limit will be detected, provided the S/N is high enough in all the bands, particularly the bluest band where an upper limit must be established. Occasionally red stellar objects and dusty galaxies contaminate the sample, but the fraction is small with high S/N images.

The only objects which might still be detectable spectroscopically, but would be missed by this technique are those with a very strong emission line and very weak continuum fluxes (typically the strong line would be $\text{Ly}\alpha$). Stockton (this volume) and Hu et al. (1999) discuss examples of such objects, and also discuss narrow-band imaging searches for detecting such objects (see also §8 below).

5. The “Madau plot” – SFR *vs* redshift

While a number of authors over the years have discussed the star formation history of the universe, one of the clearest discussions of this issue has been provided by Madau (see, e.g., Madau et al. 1996; Madau 1997; Madau, Pozzetti and Dickinson 1998). The form that was used by Madau (1997) is shown in Figure 1, and gives the star formation rate per comoving volume *vs* redshift. This was one of the early papers from Madau and shows a rise from $z \sim 5$ to $z \sim 1$ – 2 , and then a comparable drop to the present day. This form of the SFR *vs* redshift figure has become known as the “Madau plot”. If plotted versus time, instead of redshift, the star formation history is more symmetric with a clear peak around a lookback time of $\sim 60\%$ of t_0 .

However, a number of developments (e.g., dust corrections, submm results, new estimates of the SFR at low redshift) are changing the shape of the SFR *vs* time, and making the variation since $z \sim 5$ much less. For example, one of the most significant developments of the last few years has been the recognition that dust extinction is skewing our view of distant galaxies. In particular, the rest frame UV SEDs (spectral energy distributions) that are measured from optical and near-IR observations invariably have slopes indicative of modest reddening. Since

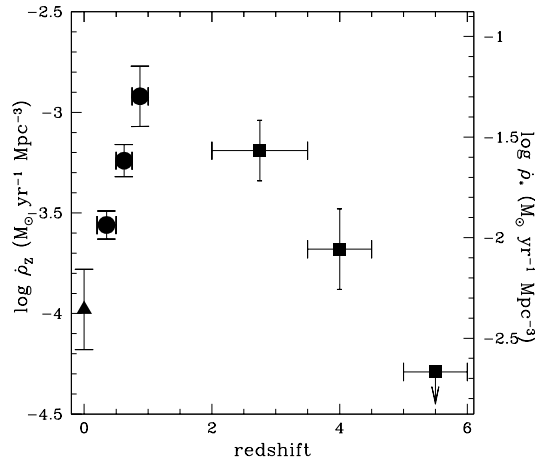


Figure 1. The star (and element) formation history of the universe, from the HDF (Madau 1997). The early data used for this figure indicated a strong peak in the SFR at about $z \sim 1-2$. See below for the form of the “Madau plot” just 2 years later.

even small amounts of reddening significantly affect the the UV fluxes that we observe the resulting corrections can be large (a factor of 2 or more). This important development will be discussed further below.

6. HST WFPC2 Imaging

The impact of HST on the field of galaxy evolution cannot be overstated. The revolution that we have witnessed in the last five years in the field of distant galaxies is due primarily to the high resolution imaging capability of the WFPC2 camera (though Keck spectroscopy has also played a key role). The morphological and structural information that can now be obtained for high redshift galaxies has placed the studies of distant galaxies onto a much more quantitative footing. So much so, that it is hard to conceive of this field without the low background, high resolution, wide-field imaging capability that we get from HST. The impact that the Hubble Deep Field (Williams et al. 1996) had on this field is well known. The number of papers generated from this tiny, five (arcmin)² region is remarkable. Even now, four years after the data were taken, it is still a joy to look at the color images of the HDF. The range in scales and morphologies of the galaxies in this

image is astonishing, as can be seen in Figure 2 (See fig2.jpg), where an expanded section of the HDF is shown.

The HDF-S added a comparable region to the southern sky opening up more opportunities for ground-based imaging (particularly JHK IR imaging) and spectroscopy (e.g., with the VLT telescopes). A number of additional fields have been imaged with HST, one of which is proving to be valuable in a quite different way. Ground-based multiobject spectrographs typically have much larger fields than the WFPC2 field, and so single HST pointings are not ideal for efficient spectroscopic followup on the ground. For example, the LRIS field on Keck covers about three contiguous WFPC2 areas, and the next generation of even wider field, multiobject spectrographs will cover more than twice the field of LRIS (e.g., DEIMOS on Keck has over $15'$ of useful field in one direction) and so 6-7 contiguous pointings in a row are really needed from HST. Thus, HST imaging surveys like the WFPC2 GTO team survey strip that has 28 contiguous WFPC2 images ($2.5' \times 42'$) in F606W (2800 s) and F814W (4200 s) are optimal for the new redshift surveys, like the Keck DEEP project (Davis and Faber 1999; Koo 1999). While not as deep as the HDF, the “Groth strip”, as the GTO team survey area is known, is proving to be an invaluable survey region. The magnitude limit for obtaining photometric and structural parameters for distant galaxies is comparable (~ 23 mag) to that for which redshifts can easily be determined using the Keck telescope and a multiobject spectrograph.

The future for HST imaging, particularly with the new wider-field, more efficient ACS, will likely be a combination of very deep, multiband images (like the HDF) for photometric redshift studies of the very faintest objects, and larger field, multiple-pointing, multiband imaging surveys (like the “Groth strip”) that can be combined with the redshifts and velocity widths determined from spectroscopic surveys with the many 6.5–10 m ground-based telescopes.

7. Galaxies at $z \sim 3$

One of the most important developments of the last decade has been the systematic study of $z \sim 3$ galaxies carried out by Steidel and his co-workers (see e.g., Steidel et al. 1996). Using largely ground-based UGR photometry to find $z \sim 3$ candidates from U-band “drop-outs” Steidel and his collaborators have obtained redshifts with Keck and confirmed some 700 $2.5 < z < 3.5$ galaxies. This is a remarkable accomplishment, when one considers that only five 5 years ago the number of known galaxies at $z > 2$ was but a handful.

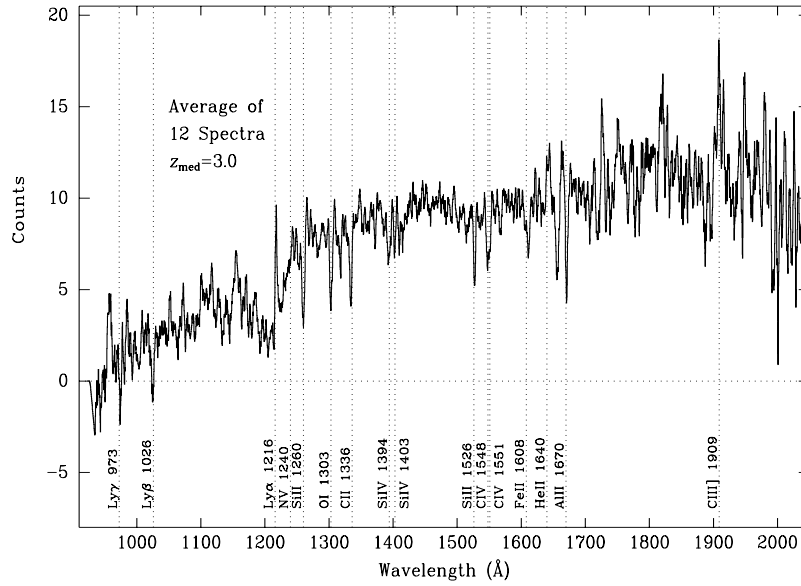


Figure 3. The composite Keck LRIS spectrum of the Lowenthal $z \sim 3$ galaxies in the HDF. Note the weak Ly α emission, the damped absorption at Ly α , the ISM and stellar wind absorption lines, and the UV continuum slope.

By extending the photometry to the red, with GRI images, Steidel et al. (1999) have obtained a sample of “blue drop-outs” (strictly G-band drop-outs, but usually referred to as “blue” as opposed to “uv” dropouts) that have already yielded a large number of $z \sim 4$ galaxies. The redshift-confirmed sample of $3.5 < z < 4.5$ galaxies is already nearly 50 objects (Steidel et al. 1999).

When HST data is available, the $z = 3-4$ galaxies can be analyzed for structural characteristics and length scales. A study that showed the value of combining redshifts with HST imaging was that of Lowenthal et al. (1997) for a small sample of $z \sim 3$ galaxies in the HDF. The composite spectrum of the galaxies that were measured with Keck is shown in Figure 3. The spectral characteristics are very similar to low redshift starbursting systems (typical SFR in this HDF sample are around $10 M_{\odot} \text{ yr}^{-1}$). The characteristic weak Ly α , as well as the many absorption lines from the ISM and stellar winds can be seen in this composite spectrum. The galaxies that have been detected in this sample (and in the Steidel et al. survey) typically have luminosities L^* or greater, and have quite small half-light radii ($\sim 0.3''$). Such measurements allow us to compare these objects with low redshift galaxies. As can be seen in Figure 4 (from Lowenthal et al. 1997), they are typically more luminous than low redshift galaxies of comparable size, but it is instructive to note that the stellar population from such a young burst will dim by

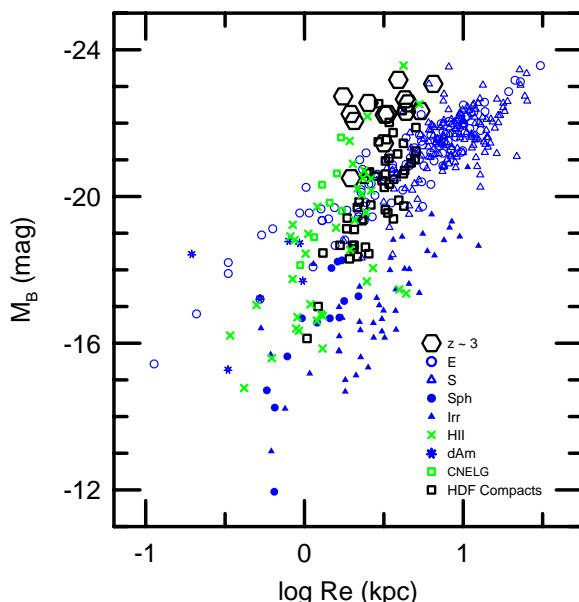


Figure 4. The absolute magnitude *vs* half-light radius for a large sample of nearby galaxies of many morphological types, overplotted with the HDF $z \sim 3$ sample (from Lowenthal et al. 1996). The $z \sim 3$ galaxies are luminous, but quite compact.

some *five* magnitudes, and so these objects could well be the precursors of local sub- L^* galaxies (of the bulges?). However, much can, and likely will happen to these objects in the 10 Gyr between $z \sim 3$ and now and so it is not obvious what such objects will become in individual cases – though since most stars will end up residing in bulges, as was noted above from the results of Fukugita, Hogan and Peebles (1998), it is almost a no-brainer to note that these are likely, on average, to be the precursors of present day bulges.

One other conclusion that can be drawn from the composite spectrum of Figure 3 is that the typical $z \sim 3$ starburst is extinguished. The slope of the UV continuum around 1500 Å can be used to estimate the level of extinction. It turns out, as might be expected, that the extinction correction is an important one, with $E(B - V)$ typically being found to be ~ 0.3 (Steidel et al. 1999). The resulting correction for the star formation rate does depend sensitively, however, on the form of the dust extinction law that is used. For example, Dickinson (1998) shows that the ratio of the mean corrected SFR to the uncorrected SFR for $z \sim 3$ galaxies was a factor 7 (!) for a Calzetti reddening law (Calzetti, Kinney and Storchi-Bergmann 1994), but only a factor 2 for an SMC reddening law, with the Calzetti law giving much greater dispersion due to its rather grey behavior. Since the Calzetti reddening

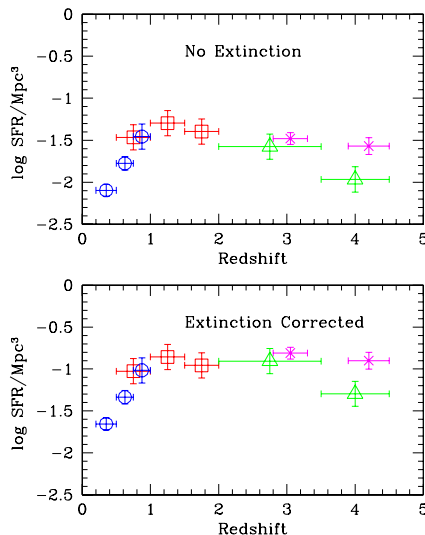


Figure 5. The recent derivation by Steidel et al. (1999) of the “Madau plot” showing the effect of using their much larger sample, and of the importance of the corrections for extinction. The HDF (lower symbols at $z = 3$ and $z = 4$) contained fewer high-redshift galaxies than the typical fields of Steidel et al., leading to an underestimate of the SFR at $z \sim 3-4$ (as in Figure 1).

law was derived for (low redshift) starburst galaxies it might seem more appropriate to use it for the high redshift starbursts, but metallicities, and the (possibly) different environment may lead one to a different reddening law – but it will be difficult to verify what the different law should be.

The net effect of both the larger sample of galaxies at high redshift and the corrections for extinction has been to raise significantly the star formation rate at $z > 2$ where the “drop-out” sample have been the dominant source of constraints on the SFR *vs* redshift. With no extinction corrections the rates have increased with the larger samples so that there is only a modest factor of 2 increase from the SFR at $z \sim 4$ to the peak SFR at $z \sim 1.5$, in contrast to the original factor of nearly an order-of-magnitude from the HDF data alone (small number statistics?). Correcting for extinction, based on a Calzetti reddening law, leads to a further increase of the SFR at redshifts $z > 2$ to where the SFR(z) relation is essentially unchanged at higher redshifts, from redshift $z \sim 4-5$ to $z \sim 1.5$. The “Madau plots” incorporating these new data are shown in Figure 5 (from Steidel et al. 1999).

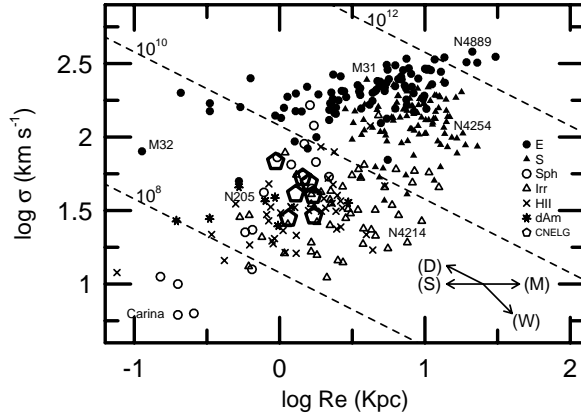


Figure 6. Half-light radius *vs* velocity width for nearby and low redshift galaxies, from Guzman et al. (1996). The corresponding mass scale are indicated by the dotted lines. The effects of various physical processes are indicated also in the lower right – see Guzman et al. for details. It is clear that a wealth of information can be derived for high redshift galaxies once they can be placed in this quantitative plane.

7.1. MASSES

One of the most important observational questions for these high redshift objects is “what are their masses?”. Masses are a crucial aspect of relating the objects we see at high redshift to those at low redshift, and for comparisons with the predictions of theoretical models. However, the strongly star-forming, compact regions that dominate in what we observe in the high redshift galaxies makes it very difficult to derive the masses of the $z \sim 3$ objects with any confidence. For example, strong outflows are seen in such objects (see, e.g., Franx et al. 1997), and so measurements of velocity widths σ from absorption, or emission lines, are likely to lead to overestimates of the gravitational masses. Yet other effects, namely dust, the small sizes of the star forming regions, etc., can lead to underestimates of the mass. It is not clear, given the limited data that we can get, even what the sense is of the overall correction, and so it has not been possible to derive reliable mass estimates from the observed velocities and length scales.

Pettini et al. (1998) and Lowenthal et al. (1998) are attempting to derive constraints on the masses, by looking at optical nebula lines, redshifted into the $2 \mu\text{m}$ region, or by using component velocity differences, but the results are still limited and very uncertain.

The value of deriving velocity and length scales in a way that is consistent with that done for low redshift galaxies is apparent from Figure 6. This figure is from Guzman et al. (1996), and compares intermediate-redshift, compact, star-forming galaxies with low redshift

galaxies, to establish their likely mass scales. Such a comparison would be very valuable to have also for high redshift galaxies.

7.2. DUST, THE UV AND THE SUBMM

As noted above the issue of dust and the extinction of the optically-detected, UV rest-frame, sources has been the subject of considerable discussion over the last few years. In parallel with efforts to characterize the impact of dust on optically-detected high redshift galaxies, a very dramatic set of results has become available over the last year on sources at high redshift that are emitting predominantly in the submm. These detections were made at $850\ \mu\text{m}$ with a new bolometer SCUBA on the 15-m JCMT telescope in Hawaii. It's large $15''$ 'beam', combined with the generally low UV and optical fluxes from these highly extincted sources, has made it hard to reliably identify the corresponding optical source and derive a redshift. A novel approach at improving the positions, by using radio continuum flux, has improved the source "identification" rate, though this may only be useful for the most luminous sources. Nonetheless, enough redshifts have been determined, which, when combined with indirect arguments, suggest that such objects could well be contributing as much (UV-equivalent) flux at high redshift as the optically-detected sources, if not more. Whether this is entirely due to starbursts, or whether AGN activity is also a contributing factor remains to be determined. However, it is likely that they are at least comparable to the optically-detected sources in their contribution to the overall SFR at high redshift, and may actually be the dominant population in the "Madau plot" at $z > 1$!

Such sources will be readily detectable with ALMA, and observable over a wide redshift range because of a shape of their SED. These sources have been detected and measured at $850\ \mu\text{m}$, which lies on the long wavelength side of the black-body distribution, such that as the redshift increases the flux increases (unlike the usual situation in the optical where the K-corrections are negative), and the increase is such as to largely cancel out the cosmological $(1+z)^4$ surface brightness dimming (see Sanders, this volume, for a good explanatory figure). Much remains to be learnt about these important new objects.

8. $z > 5$ Galaxies

Just three years ago, the first galaxy was found that had a higher redshift than the then highest redshift QSO; such an event was expected given that galaxies presumably predate QSOs, but this was the first

time since the discovery of QSOs in the 1960s that this had happened. This object was at $z = 4.92$ (Franx et al. 1997). It identified $z > 5$ as the time when we might begin to see the development of substantial baryonic potential wells. Since then, the highest redshift QSO has crept over $z = 5$, but the highest redshift galaxy has jumped to at least $z = 5.74$, and possibly even to $z = 6.68$.

The three best determined $z > 5$ objects are at $z = 5.34$ (Dey et al. 1998), $z = 5.60$ (Weymann et al. 1998), and $z = 5.74$ (Hu et al. 1999). All these redshifts were measured from Keck LRIS spectra, and all show Ly α , though all are faint with integrations ranging from 4 to 10 hours, as required to get adequate S/N in the emission line. The continuum fluxes are low, since these sources typically have I_{AB} magnitudes around 26-27, and hard to detect against the bright night sky (Ly α falls at 800 nm at $z = 5.6$). The detections are almost certainly real, since the objects are measurable in deep imaging data, and the expected flux decrements due to the continuum breaks at Ly α 1216 Å and the Lyman limit at 912 Å have been seen. In addition, the line profiles display the expected asymmetry due to blue edge absorption in Ly α in the outflowing ISM associated with the starburst (see e.g., Franx et al. 1997). The highest redshift object, at $z = 6.68$ (Chen, Lanzetta and Pascarelle 1999), is a less certain detection, given that it is faint and the data are relatively low S/N.

It is clear that we are pushing to $z \sim 6$ and beyond, but it is also clear that further progress really requires good near-IR imagers and spectrographs. At $z = 6.68$, Ly α falls at 940 nm, where typical CCDs have quite low quantum efficiency. Another interesting issue with these high redshift objects is what will we actually do with them? They are so faint that it will be extremely difficult to obtain high S/N data, even in images. As noted, they are fainter than $I_{AB} = 26$, with typical line fluxes that are very low, and, even with Keck, integrations of 4-10 hours provide little more than redshift detections. If we are to get more detailed information about such high redshift objects then a different approach must be used.

9. Strongly-Lensed Galaxies at High Redshift

Over the past few years a number of strongly-lensed distant galaxies have been found where the magnification is high enough that the source object can be studied at a level of detail that is impractical for typical galaxies at that redshift. An excellent recent example is the very good paper by Pettini et al. (1999) on the $z = 2.73$ strongly-lensed object MS 1512-cB58. Another example is the strongly-lensed object

CL 1358+62_G1 in the $z = 0.33$ cluster CL 1358+62 (Franx et al. 1997). This object is at $z = 4.92$. The large magnification ($\sim 10\times$) makes this a particularly important pathfinder for assessing the structure of galaxies at high redshifts. While it would be valuable to have other examples to enlarge the sample, this remains the best known at such a high redshift.

The cluster and its arc are shown in Figure 7 (See fig7.jpg), along with the arc prior to reconstruction, and after reconstruction into the source plane. The resolution in the reconstructed image is better than 20 milliarcsec, comparable to what one will get with adaptive optical systems on 8-10 m telescopes in the near-IR, though the sensitivity to low surface brightness extended structures will be much less in such ground-based data. This resolution corresponds to about 200 pc.

The object in the reconstructed image covers about 7 kpc, with several star forming knots interspersed throughout the galaxy. The knots dominate in that they contribute about 75% of the flux in the object, with the brightest knot alone contributing about half the flux. This corresponds to more than $10^{11} L_{\odot}$ in a single region with a half-light radius $r_{\frac{1}{2}} \sim 20$ mas or a FWHM of about 300-400 pc. The SFR implied by the observed UV flux, under the assumption of no extinction, is about $50 M_{\odot} \text{ yr}^{-1}$. However, it is clear from the combined HST optical and Keck near-IR data (Soifer et al. 1998) that the source is reddened with $E(B - V) \sim 0.3$, indicating that the SFR needs to be increased significantly to $> 10^2 M_{\odot} \text{ yr}^{-1}$, possibly $\gg 10^2 M_{\odot} \text{ yr}^{-1}$, depending on the reddening law and the dust distribution. The value of the IR data can be seen in Soifer et al. (1998) in the fits of the Bruzual and Charlot models, with Calzetti extinctions, to the measured HST WFPC2 F606W and F814W fluxes, and the Keck NIRC near-IR J, H, and K fluxes. Both the instantaneous burst and continuous star formation models need extinctions $E(B - V) \sim 0.3$ to match the observed fluxes, given the constraint that the burst must contain stars less than 10^7 yr in age so as to ensure the UV flux required for the strong Ly α .

The knot mass can be estimated from the IR luminosity, assuming a Salpeter IMF, and is $\sim 5 \times 10^9 M_{\odot}$. Given the scale size of the knot, this implies a velocity dispersion of $\sigma \sim 200 \text{ km s}^{-1}$. The size of the region, and such a velocity dispersion, is typical of many present day bulges.

Another interesting aspect of this object is that there are multiple star-forming knots within a more extended structure. This morphology is characteristic of the “christmas tree” model of star-formation in distant galaxies where different knots may “turn on” at different times, as was discussed by Lowenthal et al. (1997). A more detailed analysis

of the implications for star formation at high redshift is to be found in Illingworth et al. (2000).

10. Future Capabilities

While progress on high redshift galaxies has been quite dramatic over the last few years a number of changes are underway that will provide a similar quantum step in capability in just the next 4-5 years. The new facilities and instruments can be put into three groups.

Large Ground-Based Telescopes: — there will be roughly an order-of-magnitude increase in the number of large ground-based telescopes, from the two Keck 10-m telescopes, as the four ESO VLT 8-m telescopes are commissioned and a further 8–10 large (≥ 6.5 m) O/IR telescopes become operational (the ~ 16 are evenly split N and S). These will have efficient optical and near-IR ($\sim 1\text{--}2\ \mu\text{m}$) imagers, and multi-object spectrographs, such as DEIMOS (for Keck) and NIRMOS and VIRMOS (for the VLT), giving large throughput gains. The potential of adaptive optics for studying distant galaxies is substantial, and is part of the focus of a major new adaptive optics center funded by the NSF at the University of California, Santa Cruz – the Center for Adaptive Optics (CfAO).

Hubble Space Telescope: — there will be substantial increase in HST's capabilities, through the development of new imagers – the typical gains over current instrumentation are $>10\times$. These instruments include the wide-field CCD Advanced Camera with its SDSS filter set (as well as a large complement of narrow-band and other broad-band filters). The ACS will be launched on the HST servicing mission SM-3B in 2001. The WFC3/IR UV-IR imager that adds wide-field IR imaging capability in J and H to HST is slated for launch on the HST servicing mission SM-4 in 2004.

Submm/IR: — there will also be major developments in submm imaging, starting with upgraded SCUBA-like imagers on the JCMT, and followed by new interferometer arrays, particularly ALMA, the Atacama Large Millimeter Array. ALMA will be an extremely powerful facility for studying dusty objects over a large range of redshifts. Ultimately, NGST should allow us to directly image extremely young protogalaxies during their first major star forming events.

The key to characterizing the universe at intermediate ($z \sim 1$) and high ($z \sim 3\text{--}5+$) redshifts, and beyond, will be through extensive surveys to very weak flux levels. Such combined redshift and imaging surveys (e.g., DEEP – see Davis and Faber 1999; Koo 1999) should

produce samples with a level of statistical robustness that will be unheralded for distant galaxies.

11. Summary

As with any subject in such an infant and dynamic state there seem to be more questions than answers. For example, some key ones that intrigue me with regard to high redshift galaxies are:

(1.) — What are the physical conditions in $z \sim 3$ –4 objects, and in particular, what are their mass scale lengths, masses, and metallicities? In addition, what is the nature, location and extent of the star-forming regions in these galaxies, and what are their merging rates? What is the distribution of the dust, and can we characterize the dynamical conditions and the extent of the outflows in the ISM that envelopes their star-forming regions?

(2.) — What are the properties of the youngest objects that we see, those at $z > 5$? Again, what are their metallicities, their mass scale lengths and their masses, and what is their space density and luminosity function? The strong Ly α lines, relative to the continuum, in contrast to the $z \sim 3$ –4 galaxies suggests that they are less dusty, but is this a selection effect? How much dust do “typical” $z > 5$ objects contain?

(3.) — What is the integrated SFR from $z \sim 5$ to $z \sim 1$ in the dust-enshrouded (submm) sources? How does it compare to the integrated SFR seen in the optical-UV (when corrections have been applied for the more modest dust-absorption typically found in these optically-detected sources)?

(4.) — Are we missing a whole set of objects with higher reddening/extinction than the typical $E(B - V) \sim 0.2 - 0.3$ sources found in the $z \sim 3$ –4 “drop-out” sample, but which would not contain enough dust to be detectable at 850 μm with SCUBA?

(5.) — What is the form of the extinction at high redshift – and can it be characterized by a single reddening law?

These questions notwithstanding, we have made substantial progress over the last few years. Given that few galaxies were known at redshifts $z > 2$ just five years ago, it is remarkable that we now can identify the time evolution of the star-formation rate in galaxies from redshifts $z \sim 5$ through to the present day. Many uncertainties remain, particularly with regard to the overall contribution from the dust-enshrouded submm sources, but the most likely situation is that by $z \sim 5$, within 1-2 Gyr of recombination, the SFR per comoving volume element had

reached a level comparable to that at all redshifts down to $z \sim 1$, after which it decreased somewhat to the present day.

Interestingly, very simple arguments based on the census of the baryons at the present day, the ages of the stellar populations in ellipticals (see e.g., van Dokkum et al. 1998), plus the sizes and densities of the star forming regions at $z \sim 2 - 5$ suggest that most of the star formation we see at $z > 2$ is making bulges.

Acknowledgements

I would like to acknowledge many valuable discussions with numerous colleagues – the remarkable progress over the last few years is due to the imagination and energy of many in our small community who have worked so hard to bring us state of the art facilities that open up new horizons. Their efforts, and those who use them imaginatively to further our understanding, and those who model the results and provide the theoretical underpinnings together make it a delight to be part of this field. I am also particularly grateful to those in our funding agencies and national centers who work, often under great pressure, to bring us the facilities and funding that allows our community to reach far and to do it so rapidly. Last but most importantly, this was a timely and fascinating conference and I am very grateful to our energetic organizer, David Block, for an excellent conference, and to Margi Crookes for her dedication to making everything work well, and to all those who helped them. The financial support from the Anglo-American Chairman's Fund and SASOL was essential to making this such a successful conference, and I would particularly like to thank those organizations.

References

- D. Calzetti, A. L. Kinney, and T. Storchi-Bergmann. Dust Extinction of the Stellar Continua in Starburst Galaxies: The Ultraviolet and Optical Extinction Law. *Astrophysical Journal*, 429, 582, 1994.
- H. -W. Chen, K. M. Lanzetta, and S. Pascarelle. Spectroscopic identification of a galaxy at a probable redshift of $z = 6.68$. *Nature*, 398, 586, 1999.
- Marc Davis and S. M. Faber. The DEIMOS Spectrograph and a Planned DEEP Redshift Survey on the Keck-II Telescope. In the 14th IAP Colloquium *Wide Field Surveys in Cosmology*, eds. S. Colombi, Y. Mellier and B. Raban (Gif-sur-Yvette: Editions Frontieres), 333, 1999.
- Arjun Dey, Hyron Spinrad, Daniel Stern, James R. Graham, and Frederic H. Chaffee. A Galaxy at $z = 5.34$. *Astrophysical Journal*, 498, L93, 1998.

- M. Dickinson. Color-Selected High Redshift Galaxies and the HDF. In the STScI Symposium Series 11 *The Hubble Deep Field*, eds. M. Livio, S. M. Fall and P. Madau (Cambridge University Press), 219, 1998.
- M. Franx, G. D. Illingworth, Daniel D. Kelson, Pieter G. van Dokkum, and Kim-Vy Tran. A Pair of Lensed Galaxies at $z = 4.92$ in the Field of CL1358+62. *Astrophysical Journal*, 486, L75, 1997.
- M. Fukugita, C. J. Hogan, and P. J. E. Peebles. The Cosmic Baryon Budget. *Astrophysical Journal*, 503, 581, 1998.
- Rafael Guzman, David C. Koo, S. M. Faber, Garth D. Illingworth, Marianne Takamiya, Richard G. Kron, Matthew A. Bershadsky. On the Nature of the Faint Compact Narrow Emission-Line Galaxies: The Half-Light Radius-Velocity Width Diagram. *Astrophysical Journal*, 460, L5, 1996.
- Esther M. Hu, Richard G. McMahon, and Lennox L. Cowie. An Extremely Luminous Galaxy at $z = 5.74$. *Astrophysical Journal*, 522, 9, 1999.
- Garth D. Illingworth et al. Star Formation at $z \sim 5$: The Lensed $z = 4.92$ Galaxy CL 1358+62-G1. *In Preparation*.
- David C. Koo. Pre-DEIMOS Pilot Surveys for DEEP. In the 14th IAP Colloquium *Wide Field Surveys in Cosmology*, eds. S. Colombi, Y. Mellier and B. Raban (Gif-sur-Yvette: Editions Frontieres), 161, 1999.
- S. J. Lilly, L. Tresse, F. Hammer, David Crampton, and O. Le Fevre. The Canada-France Redshift Survey. VI. Evolution of the Galaxy Luminosity Function to $z \sim 1$. *Astrophysical Journal*, 455, 108, 1995.
- James D. Lowenthal, David C. Koo, Rafael Guzman, Jesus Gallego, Andrew C. Phillips, Nicole P. Vogt, S. M. Faber, Garth D. Illingworth, and Caryl Gronwall. Keck Spectroscopy of Redshift $z \sim 3$ Galaxies in the Hubble Deep Field. *Astrophysical Journal*, 481, 673, 1997.
- J. D. Lowenthal, L. Simard, and D. C. Koo. Kinematics of Galaxies at $z \sim 3$ in the Hubble Deep Field. In the Proceedings of *The Young Universe: Galaxy formation and Evolution at Intermediate and High Redshift* eds S. D'Odorico, A. Fontana, and E. Giallongo (San Francisco: ASP) ASP Conference Series, 146, 110, 1998.
- Piero Madau, Henry C. Ferguson, Mark E. Dickinson, Mauro Giavalisco, Charles C. Steidel, and Andrew Fruchter. High-Redshift Galaxies in the Hubble Deep Field: Color Selection and Star Formation History to $z \sim 4$. *Monthly Notices of the Royal Astronomical Society*, 283, 1388, 1996.
- Piero Madau, Lucia Pozzetti, and Mark Dickinson. The Star Formation History of Field Galaxies. In the Seventh Astrophysics Conference *Star Formation Near and Far*, eds Steven S. Holt and Lee G. Mundy (Woodbury N. Y. : AIP Press) AIP Conference Series, 393, 481, 1997.
- Piero Madau. Cosmic Star Formation History. *Astrophysical Journal*, 498, 106, 1998.
- Max Pettini, Melinda Kellog, Charles C. Steidel, Mark Dickinson, Kurt L. Adelberger, and Mauro Giavalisco. Infrared Observations of Nebular Emission Lines from Galaxies at $z = 3$. *Astrophysical Journal*, 508, 539, 1998.
- Max Pettini, Charles C. Steidel, Kurt L. Adelberger, Mark Dickinson, and Mauro Giavalisco. The Ultraviolet Spectrum of MS 1512-cB58: An Insight into Lyman Break Galaxies. *Astrophysical Journal*, in press, 1999.
- B. T. Soifer, G. Neugebauer, M. Franx, K. Matthews, and G. D. Illingworth. Near-Infrared Observations of a Redshift 4.92 Galaxy: Evidence for Significant Dust Absorption. *Astrophysical Journal*, 501, L171, 1998.

- Charles C. Steidel, Mauro Giavalisco, Max Pettini, Mark Dickinson, and Kurt L. Adelberger. Spectroscopic Confirmation of a Population of Normal Star-Forming Galaxies at Redshifts $z > 3$. *Astrophysical Journal*, 462, L17, 1996.
- Charles C. Steidel, Kurt L. Adelberger, Mark Dickinson, Mauro Giavalisco, Max Pettini, and Melinda Kellog. A Large Structure of Galaxies at Redshift $z \sim 3$ and Its Cosmological Implications. *Astrophysical Journal*, 492, 428, 1998.
- Charles C. Steidel, Kurt L. Adelberger, Mauro Giavalisco, Mark Dickinson, and Max Pettini. Lyman-Break Galaxies at $z > 4$ and the Evolution of the Ultraviolet Luminosity Density at High Redshift. *Astrophysical Journal*, 519, 1, 1999.
- Pieter G. van Dokkum, Marijn Franx, Daniel D. Kelson, and Garth D. Illingworth. Luminosity Evolution of Early-Type Galaxies to $z = 0.83$: Constraints on Formation Epoch and Omega. *Astrophysical Journal*, 504, L17, 1998.
- Ray J. Weymann et al. Keck Spectroscopy and NICMOS Photometry of a Redshift $z = 5.60$ Galaxy. *Astrophysical Journal*, 505, L95, 1998.
- Robert E. Williams et al. The Hubble Deep Field: Observations, Data Reduction, and Galaxy Photometry. *Astronomical Journal*, 112, 1335, 1996.

